Performance Analysis of Large Multiuser MIMO Systems With Space-Constrained 2-D Antenna Arrays

Performance Analysis of Large Multi-User MIMO Systems with Space-Constrained 2D Antenna Arrays

Sudip Biswas, *Christos Masouros*, *Senior Member, IEEE* and *Tharmalingam Ratnarajah*, *Senior Member, IEEE*

***Abstract*—Massive Multiple-Input-Multiple-Output (MIMO) systems deploying a large number of antennas at the base station (BS) have been shown to produce high spectral and energy efficiency (EE) under the assumptions of increasing BS physical space and critical antenna spacing. We examine the deployment of massive MIMO systems and resulting EE with a more realistic scenario considering a 2D rectangular array with increasing antenna elements within a fixed physical space. Mutual coupling and correlation among the BS antennas are incorporated by deriving a practical mutual coupling matrix which considers coupling among all antenna elements within a BS. We also provide a realistic analysis of the energy consumption using a model, which takes into account the circuit power consumptions as a function of the number of BS antennas and then present a performance analysis of two practical low complexity detectors/receivers keeping EE into consideration. The simulation results obtained show that EE does not monotonically increase with the number of BS antennas. On the contrary, it is a decreasing concave or quasi-concave function of the number of BS antennas depending on the detection technique used at the receiver. We also show that with decreasing spacing between the antennas, mutual coupling increases, contributing towards reduction in EE. Our analysis thus shows that EE does not increase infinitely in a massive MIMO system when the increasing number of antennas are to be accommodated within a fixed physical space and the total power consumed is considered to be a function of the antennas. Accordingly, closed-form expressions for the optimum number of antennas to attain maximum EE for zero forcing (ZF) are obtained.**

***Index Terms*—Antenna correlation, antenna coupling, energy efficiency, massive MIMO, spectral efficiency.**

I. Introduction

To meet the ever-increasing demands for the next generation of wireless communication, massive Multiple-Input-Multiple-Output (MIMO) systems are introduced based on the fact that the BS is equipped with a much larger number of antennas than the number of users served [1], [2] which enable us to design simple signal processing algorithms [2] that can attain very high spectral efficiency [3]. Such systems are now being implemented in various wireless communication technologies such as LTE-Advanced [4] and 802.11n [5] to name a few. However, due to the limited availability of wireless spectrum, massive MIMO can be truly exploited only by significantly increasing the number of antennas deployed per unit area [6]. A usual practice when deploying antenna elements is to space them by a distance equal to wavelength of the transmitted frequency or more [1], [7]. One of the constraints towards this end is the limited availability of physical area for deployment of large number of antennas at the base station. Massively densified antenna deployment is a way out but it leads to two effects, namely spatial correlation and antenna mutual coupling. The proximity of the antenna elements as signal sources and electrical components causes antenna correlation and coupling respectively [8].

The nulls and the maximum of the radiation pattern of the antennas are shifted owing to the mutual coupling among them [9]. Mutual coupling effects among antenna elements in 1D linear arrays have widely been studied in [10]-[15]. While [10] and [11] focus on the performance of adaptive arrays when exerted to mutual coupling, [8] and [17] examine the performance of massive MIMO systems with antenna elements affected by mutual coupling owing to constrained physical space. Mutual coupling due to constrained antenna spacing has been stated to deteriorate the performance of MIMO systems by influencing the correlation of the antennas in [18], [19]. Effects of mutual coupling on the radiation patterns of phased arrays were investigated in [20]. Effects of transmit correlation and mutual coupling on linear precoders were analyzed considering large scale MIMO transmitters in [8]. While a considerable amount of work has already been done with regards to antenna coupling in MIMO, its effects are still quite unknown when a massive MIMO scenario with hundreds of antennas at the BS are considered. Also to be noted is that most prior work on effects of antenna coupling on MIMO is based on linear arrays [11]-[13]. Since the need of the hour is to accommodate as many number of antennas as possible, we present a more realistic 2D rectangular antenna array configuration with antennas increasing upto 250. If antenna elements are rigged considering a spacing less than half the wavelength of transmission, a considerable number of antennas will be coupled affecting both the spectral efficiency (SE) and

S. Biswas and T. Ratnarajah are with the Institute for Digital Communications, The University of Edinburgh, King's Buildings, Edinburgh, EH9 3JL, UK, (e-mail: {sudip.biswas, t.ratnarajah}@ed.ac.uk).

C. Masouros is with Dept. of Electronic and Electrical Engineering, University College London, Torrington Place, London, WCEI 7JE, UK, (e-mail: chris.masouros@ieee.org).

This work was supported by the UK Engineering and Physical Sciences Research Council (EPSRC) under grant number EP/L025299/1 and the Royal Academy of Engineering, UK. The work of S. Biswas was also supported by the Seventh Framework Programme for Research of the European Commission under grant number HARP-318489.

This article has been accepted for publication in a future issue of this journal, but has not been fully edited. Content may change prior to final publication. Citation information: DOI 10.1109/TWC.2016.2522419, IEEE Transactions on Wireless Communications

energy efficiency (EE) of the system. While mutual coupling models for 2D antenna arrays have been ever-present in the field of communications, most existing works on large-scale MIMO systems predict over-optimistic performance assuming arrays with unbounded physical space, the more relevant work in [8] considers only linear arrays and a simplified mutual coupling model. In this work, we consider a more realistic 2D planar array bounded by a fixed physical space with an area of about $1m^2$ and analytically account for the full mutual coupling model of the array.

Any new system developed in the field of communication would demand energy saving as one of its primary design criteria. The advent of technology hasn't actually reduced the energy consumption of the BS and user equipments (UE); instead energy consumption and power radiation has become a major health and economic hazard over the years [5]. [28] discusses the electrical power consumptions of the power amplifiers, the cooling systems and the associated circuits installed at the BS. While large antenna arrays have been stated to reduce uplink (UL) and downlink (DL) transmit powers due to coherent combining and an increased antenna aperture in [29], [3] claims such systems operate with a total output RF power of magnitude which is two times less than the current technology. Thus, with the emergence of massive MIMO, we can claim to have taken a giant leap towards reducing the consumption of energy in the field of communication. But how massive is the leap and where will it lead us towards conservation of energy? We will try to analyse this question with respect to EE that can be considered to be a very proficient design goal when it comes to developing energy efficient communication systems.

EE of a communication link is usually defined as the total energy required for transmission in order to achieve a specific SE [21], [1]. The significance of the total power consumption in MIMO systems has been emphasized in [22] with respect to EE. MIMO systems have been stated to offer improved EE on account of array gains and diversity effects [33]. A common practice in determining EE is to consider the total transmitted energy to be a constant quantity [1] which aids in reducing the complexity of calculations. Hence, the definition of EE can be quite delusive at times especially when a massive MIMO scenario is considered with the number of antennas increasing asymptotically leading towards unbounded EE which is quite improbable for practical scenarios. The effect of number of BS antennas on EE has been discussed in [5] and [23], while [24] discusses about designing optimal EE for the uplink massive MIMO systems considering both RF and circuit power consumptions. In [30] power optimization techniques were analyzed using Game theory approaches while considering both circuit and transmission powers. A trade-off between the EE and SE was also given in [30].

The focus of this paper is to consider realistic setups of massive MIMO and analyze how large MIMO systems bounded by fixed physical spaces fare to the demands of increasing EE while contributing towards high spectral efficiencies. We re-examine the question- "How many antennas do we need?"

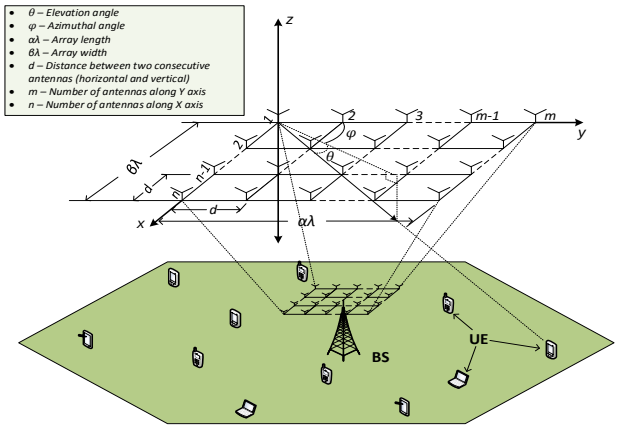

Fig. 1: An illustration of a multi-user MIMO setup- A 2D rectangular array consisting of M dipole antennas serving K single-antenna users located uniformly within the cell diameter in the uplink and downlink.

[2] by means of EE under a) realistic antenna deployments in fixed physical spaces and b) thorough and pragmatic power consumption models. We reflect on both the uplink and downlink of a multi-user MIMO system which models antenna correlation and coupling at the BS. We calculate the SE and transmitted power for both uplink and downlink and also the EE of this system with the help of a power consumption model similar to [24], incorporating parameters like power consumed by amplifiers and other digital circuits. Our analysis is based on the effect of increasing the number of BS antennas and reducing the antenna spacing on the EE of the system while taking into consideration two practical linear receivers/precoders in maximum ratio combining/transmission (MRC/MRT) and zero forcing (ZF). To obtain a fair comparison, we analyze the EE of massive MIMO systems considering the fixed power consumption for the cases of two current communication technologies- WIFI and LTE. While analytical expression for EE is obtained for ZF only, simulation results are provided for both MRC and ZF. The results provide adequate insights into how future massive MIMO Base stations can be setup within constrained physical spaces.

Notation: All matrices and vectors will be represented in bold uppercase and lowercase symbols respectively while $(.)^T$ and $(.)^H$ are used to denote the transpose and Hermitian transpose of a matrix respectively. E is used to denote the expectation operator. All other symbols will be explicitly mentioned wherever used.

II. System Model

We consider the uplink and downlink of a single cell multi-user MIMO arrangement with one BS equipped with a uniform rectangular 2D antenna array located in a fixed physical space of area Δ. Each row and column of the antenna array consists of n and m dipole antennas respectively with each element separated from the other by a distance d within a row or a

column. $M = n \times m$ is the total number of antennas receiving signals from K single-antenna users with $M \gg K$. The users are assumed to transmit their data in the same time-frequency resource with λ being the carrier wavelength. We also assume that $d < \lambda/2$ so that antenna coupling significantly impacts the performance of the system. Furthermore the length and breadth of the rectangular array are $\alpha\lambda$ and $\beta\lambda$ $(\alpha, \beta \in \mathbb{N})$ respectively which leads to the following expressions

$$\Delta = \alpha\beta\lambda^2, \tag{1}$$

$$d = \frac{\alpha\lambda}{m-1} = \frac{\beta\lambda}{n-1}. \tag{2}$$

Hereinafter, any analysis performed with respect to the $n \times m$ rectangular array will take into consideration the following assumptions-

a) The antenna elements are placed at uniform intervals.
b) All the elements are identical to each other. In our case we consider dipoles of equal length.
c) All the elements have equal amplitude excitation.
d) The directions of arrivals (DOAs) or directions of departures (DODs) are randomly and independently distributed in angle spread ϕ as a (D, ϕ) channel (D is explained later).

Perfect synchronization in time and frequency is considered between the BS and users, which operate in a time division duplex (TDD) protocol. The uplink and downlink channels are assumed to be reciprocal within a coherence block. Moreover, the uplink and downlink transmissions follow a ratio Υ^{UL} : Υ^{DL} where Υ^{UL} and Υ^{DL} are fixed transmission ratios for uplink and downlink respectively [7] with $\Upsilon^{UL} + \Upsilon^{DL} = 1$. Let T be the length of the coherence time interval and τ^{UL}, τ^{DL} are the number of symbols used for uplink and downlink pilots respectively. Uplink training utilizes $K\tau^{UL}$ of the coherence time interval while downlink training occupies $K\tau^{DL}$. The BS utilizes the uplink training to estimate the downlink channel.

Let $\mathbf{W}$ represent a semi-correlated frequency-flat channel matrix between the BS and the K users which is modeled as $\mathbf{W} = \mathbf{H}\mathbf{F}^{\frac{1}{2}}$ for uplink with $\mathbf{H} \sim \mathcal{CN}(\mathbf{0}, \mathbf{\Sigma}_M^{UL} \otimes \mathbf{I}_K)$ representing the uplink channel and $\mathbf{W} = \mathbf{F}^{\frac{1}{2}}\mathbf{H}$ for downlink with $\mathbf{H} \sim \mathcal{CN}(\mathbf{0}, \mathbf{I}_K \otimes \mathbf{\Sigma}_M^{DL})$[1] representing the downlink channel, where $\mathbf{\Sigma}_M^{UL} = \mathbf{\Sigma}_M^{DL} = \mathbf{\Sigma}_M$ is the BS correlation matrix, $\otimes$ denotes the Kronecker product operator and $\mathbf{F}$ is a $K \times K$ diagonal matrix, where $[\mathbf{F}_{kk}] = \beta_k$. $\sqrt{\beta_k}$ models the geometric attenuation and shadow fading which is assumed to be independent over M and constant over several coherence time intervals. This holds true owing to the assumption that $d \ll r_u$, where r_u is the minimum distance between an arbitrary user and the BS and β_k changes very slowly with time.

[1]It is to be noted that for simplicity of notation, we represent the uplink and downlink channel matrix with the same notation. However, wherever used, its property will be clearly mentioned.

A. Channel Model with Correlation and Coupling

We examine a single-cell setup with an M-antenna BS and K single-antenna users. The uplink and downlink channels are modeled as one-sided correlated Rayleigh flat fading channel with no line of sight. We assume the fading to be correlated only at the BS [25]. After incorporating the mutual coupling of the receiving antennas, we model $\mathbf{H}$ for uplink as [8]

$$\mathbf{H} = \begin{bmatrix} \mathbf{h}_1, & \dots & \mathbf{h}_k, & \dots & \mathbf{h}_K \end{bmatrix}, \tag{3}$$

where $\mathbf{h}_k$ is the $M \times 1$ uplink channel vector of the k-th user; given as

$$\mathbf{h}_k = \mathbf{\Gamma}\mathbf{A}_k^{UL}\mathbf{g}_k \tag{4}$$

and for downlink as

$$\mathbf{H} = \begin{bmatrix} \mathbf{h}_1^T, & \dots & \mathbf{h}_k^T, & \dots & \mathbf{h}_K^T \end{bmatrix}^T, \tag{5}$$

where $\mathbf{h}_k$ is the $1 \times M$ downlink channel vector of the k-th user; given as

$$\mathbf{h}_k = \mathbf{g}_k\mathbf{A}_k^{DL}\mathbf{\Gamma}, \tag{6}$$

where $\mathbf{\Gamma} \in \mathbb{C}^{M \times M}$ denotes mutual coupling, $\mathbf{A}_k^{UL} \in \mathbb{C}^{M \times D}$ denotes the receive steering matrix during uplink containing D steering vectors of the receive antenna array with D denoting the number of direction of arrivals (DOAs) while $\mathbf{A}_k^{DL} \in \mathbb{C}^{D \times M}$ denotes the transmit steering matrix during downlink containing D steering vectors of the receive antenna array with D denoting the number of direction of departures (DODs) and the vector $\mathbf{g}_k \sim \mathcal{CN}(\mathbf{0}, \mathbf{I}_D)$ whose dimensions for uplink and downlink are $D \times 1$ and $1 \times D$ respectively. For the sake of simplicity, the number of DOAs and DODs are considered to be equal. Furthermore, for the uplink transmission, $[\mathbf{H}^H\mathbf{H}] \sim \mathcal{CW}_K(M, \mathbf{\Sigma}_M)$ where $\mathcal{CW}_q(r, \mathbf{S})$ denotes a complex Wishart distribution with degrees of freedom r, dimension q and covariance $\mathbf{S}$. Similarly for downlink transmission, $[\mathbf{H}\mathbf{H}^H] \sim \mathcal{CW}_K(M, \mathbf{\Sigma}_M)$.

B. Channel Correlation at the Transmitter

We consider the antenna array at the BS to be uniformly rectangular as shown in Fig. 1. As stated before, the spacing between two adjacent antennas within a row or a column is considered to be d. Thus without loss of generality, the steering matrix with respect to the ith direction of arrival can then be expressed as [16]

$$\mathbf{A}_i = \mathbf{a}_c(\phi_i, \theta)\mathbf{a}_r(\phi_i, \theta)^T, \tag{7}$$

where $\mathbf{a}_c(\theta, \phi) \in \mathbb{C}^{n \times 1}$ is the column array steering vector given as

$$\mathbf{a}_c(\phi_i, \theta) = \left[1, e^{j\frac{2\pi}{\lambda}d\cos\phi_i\sin\theta}, \dots, e^{j\frac{2\pi}{\lambda}d(n-1)\cos\phi_i\sin\theta}\right]^T \tag{8}$$

and $\mathbf{a}_r(\theta, \phi) \in \mathbb{C}^{m \times 1}$ is the row array steering vector given as

$$\mathbf{a}_r(\phi_i, \theta) = \left[1, e^{j\frac{2\pi}{\lambda}d\sin\phi_i\sin\theta}, \dots, e^{j\frac{2\pi}{\lambda}d(m-1)\sin\phi_i\sin\theta}\right]^T. \tag{9}$$

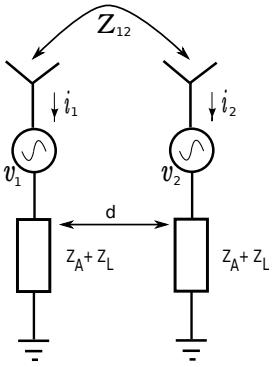

Fig. 2: An illustration showing the effect of mutual coupling on two dipole antennas located adjacent to each other spaced at d distant apart.

Using the vector valued operator vec$\{\cdot\}$, which maps a $m \times n$ matrix to a $mn \times 1$ column vector by stacking the columns of the matrix, the array steering matrix may be transformed to a 2-D array steering vector as

$$\mathbf{a}(\phi_i, \theta) = \text{vec}\{\mathbf{A}_i\}. \tag{10}$$

The $M \times D$ steering matrix of the rectangular array for uplink can now be given as

$$\mathbf{A}^{UL} = [\mathbf{a}(\phi_1, \theta), \ldots, \mathbf{a}(\phi_i, \theta), \ldots, \mathbf{a}(\phi_D, \theta)], \tag{11}$$

where $\mathbf{a}(\phi_i, \theta) \in \mathbb{C}^{M \times 1}$ for $i \in 1, 2, 3 \ldots, D$. Similarly for downlink the $D \times M$ steering matrix is given as

$$\mathbf{A}^{DL} = [\mathbf{a}(\phi_1, \theta)^T, \ldots, \mathbf{a}(\phi_i, \theta)^T, \ldots, \mathbf{a}(\phi_D, \theta)^T]^T. \tag{12}$$

Hereinafter, for notational simplicity, we represent the uplink and downlink steering matrix with the same notation $\mathbf{A}$. However, the property of the matrix will be clearly mentioned, wherever used. Throughout this paper we consider d to be equidistant and the D DOAs and DODs are randomly and independently distributed in an angle spread determined by the azimuth $\phi_i \in [-\frac{\pi}{2}, \frac{\pi}{2}], i = 1, 2, 3 \ldots, D$ and the same elevation $\theta \in [-\frac{\pi}{2}, \frac{\pi}{2}]$. Different degrees of transmit correlation are obtained by varying ϕ of the semi-correlated (D, ϕ) channel.

C. Mutual Coupling at the Transmitter

When multiple antennas radiating simultaneously are located in the proximity of each other within a fixed physical space, the electric field of one antenna impacts the distribution of current of the adjacent antennas, which leads to the radiation pattern and input impedance of each antenna being disturbed [18]. This phenomenon is known as antenna coupling.

Our system model is characterized by mutual coupling among linear dipole antennas of length l which are arranged in a planar configuration with uniform square grids and rectangular boundary as shown in Fig. 1 and described earlier. The mutual coupling matrix, $\mathbf{\Gamma}$ is defined as [9]

$$\mathbf{\Gamma} = (Z_L + Z_A)(\mathbf{Z} + Z_L \mathbf{I})^{-1}, \tag{13}$$

where Z_L, Z_A and $\mathbf{Z}$ denote load impedance, antenna impedance and mutual impedance matrix respectively. $\mathbf{Z}$ can be constructed as a $M \times M$ matrix, which is given in (14) on top of the following page, where $Z_{(i,k)(j,l)}$ denotes the mutual impedance between antenna located at the ith row and kth column and the antenna located at the jth row and lth column of the rectangular array with $i, j \in 1, 2, \ldots, n$ and $k, l \in 1, 2, \ldots, m$.

The correlation matrix at the BS for uplink can be given as

$$\begin{aligned} \mathbf{\Sigma}_M^{UL} &= E\{\mathbf{H}\mathbf{H}^H\} \\ &= \mathbf{\Gamma}\mathbf{A}E\{\mathbf{g}_k\mathbf{g}_k^H\}\mathbf{A}^H\mathbf{\Gamma}^H \\ &= K\mathbf{\Gamma}\mathbf{A}\mathbf{A}^H\mathbf{\Gamma}^H. \end{aligned} \tag{15}$$

Similarly, the correlation matrix at the BS for downlink is given as

$$\mathbf{\Sigma}_M^{DL} = K\mathbf{\Gamma}^H\mathbf{A}^H\mathbf{A}\mathbf{\Gamma}. \tag{16}$$

Since $\mathbf{\Sigma}_M^{UL} = \mathbf{\Sigma}_M^{DL} = \mathbf{\Sigma}_M$, we will ignore the superscripts UL and DL henceforth.

Example 1. Assume that the antennas at the BS are rigged in a uniform planar array with square grids and rectangular boundary as shown in Fig. 1 and Fig. 2. Applying simple algebraic operations on the Cartesian co-ordinates of the rectangular array, the distance between any two antenna elements within the array can be given as

$$d_{(i,k)(j,l)} = d\sqrt{(i-j)^2 + (k-l)^2}, \tag{17}$$

where i, j, k, l are described as before.

$d_{(i,k)(j,l)}$ plays a significant role in determining the mutual impedance, $Z_{(i,k)(j,l)}$ which based on current maximum at the input antenna terminal is given by the EMF method as [4]

$$Z_{(i,k)(j,l)} = R_{(i,k)(j,l)} + \mathrm{j}X_{(i,k)(j,l)}, \tag{18}$$

where, $R_{(i,k)(j,l)}$ and $X_{(i,k)(j,l)}$ are self-mutual-resistance and self-mutual-reactance between antenna located at the ith row and kth column and the antenna located at the jth row and lth column respectively and given as [9]

$$R_{(i,k)(j,l)} = \frac{\sqrt{\mu_0}}{4\pi\sqrt{\epsilon_0}} \left[2C_{in}(u_0) - C_{in}(u_1) - C_{in}(u_2)\right] \tag{19}$$

and

$$X_{(i,k)(j,l)} = \frac{\sqrt{\mu_0}}{4\pi\sqrt{\epsilon_0}} \left[2S_{in}(u_0) - S_{in}(u_1) - S_{in}(u_2)\right], \tag{20}$$

where μ_0 and ϵ_0 denote the magnetic and electric constants, $u_0 = 2\pi d_{(i,k)(j,l)}$, $u_1 = 2\pi\left(l + \sqrt{d_{(i,k)(j,l)}^2 + l^2}\right)$ and $u_2 = 2\pi\left(-l + \sqrt{d_{(i,k)(j,l)}^2 + l^2}\right)$. $C_{in}(.)$ and $S_{in}(.)$ are cosine and sine integral functions respectively and defined as

$$C_{in}(a) = \gamma + \ln(a) + \int_0^a \frac{\cos t - 1}{t} dt, \tag{21}$$

$$S_{in}(a) = \int_0^a \frac{\sin t}{t} dt, \tag{22}$$

where γ is the Euler-Mascheroni constant and l is the length

This article has been accepted for publication in a future issue of this journal, but has not been fully edited. Content may change prior to final publication. Citation information: DOI 10.1109/TWC.2016.2522419, IEEE Transactions on Wireless Communications

$$\mathbf{Z} = \begin{bmatrix} Z_{(1,1)(1,1)} & \cdots & Z_{(1,1)(1,m)} & \cdots & Z_{(1,1)(2,1)} & \cdots & Z_{(1,1)(2,m)} & \cdots & Z_{(1,1)(n,1)} & \cdots & Z_{(1,1)(n,m)} \\ Z_{(1,2)(1,1)} & \cdots & Z_{(1,2)(1,m)} & \cdots & Z_{(1,2)(2,1)} & \cdots & Z_{(1,2)(2,m)} & \cdots & Z_{(1,2)(n,1)} & \cdots & Z_{(1,2)(n,m)} \\ \vdots & \ddots & \vdots & \ddots & \vdots & \ddots & \vdots & \ddots & \vdots & \ddots & \vdots \\ Z_{(1,m)(1,1)} & \cdots & Z_{(1,m)(1,m)} & \cdots & Z_{(1,m)(2,1)} & \cdots & Z_{(1,m)(2,m)} & \cdots & Z_{(1,m)(n,1)} & \cdots & Z_{(1,m)(n,m)} \\ \vdots & \ddots & \vdots & \ddots & \vdots & \ddots & \vdots & \ddots & \vdots & \ddots & \vdots \\ Z_{(n,1)(1,1)} & \cdots & Z_{(n,1)(1,m)} & \cdots & Z_{(n,1)(2,1)} & \cdots & Z_{(n,1)(2,m)} & \cdots & Z_{(n,1)(n,1)} & \cdots & Z_{(n,1)(n,m)} \\ \vdots & \ddots & \vdots & \ddots & \vdots & \ddots & \vdots & \ddots & \vdots & \ddots & \vdots \\ Z_{(n,m)(1,1)} & \cdots & Z_{(n,m)(1,m)} & \cdots & Z_{(n,m)(2,1)} & \cdots & Z_{(n,m)(2,m)} & \cdots & Z_{(n,m)(n,1)} & \cdots & Z_{(n,m)(n,m)} \end{bmatrix} \quad (14)$$

of the dipole antenna.

The electrical and magnetic parameters of the antennas are considered to be equal for every antenna. Hence, considering equal spacing among the antennas along row and column of the rectangular array, the following properties for the mutual impedance matrix $\mathbf{Z}$ can be obtained -

a) $\mathbf{Z}$ is a symmetric. Let Z_{uv} be the element in the uth row and vth column of $\mathbf{Z}$. Then
$$Z_{uv} = Z_{vu}. \quad (23)$$
b) $\mathbf{Z}$ is a Toeplitz matrix. Thus
$$Z_{uv} = Z_{(u+1)(v+1)}. \quad (24)$$
c) $\mathbf{Z}$ has $2M-1$ degrees of freedom.

Remark 1. Let $Z_{pq} = Z_{(i,k)(j,l)}$, where $p, q \in 1, 2, \ldots, M$. If $p = q$, then $\Gamma_{pq} = Z_A$, where Z_A denotes antenna or self impedance.

III. Spectral Efficiency and Transmitted Power

A. Uplink

During uplink transmission, the K users transmit their data in the same time-frequency resource. Thus the $M \times 1$ received vector at the BS can be given as
$$\mathbf{y} = \mathbf{W}\mathbf{P}^{UL}\mathbf{x} + \mathbf{z}, \quad (25)$$
where $\mathbf{x} \in \mathbb{C}^{K\times 1}$ is the symbol transmitted by the K users. $\mathbf{P}^{UL}$ is a $K \times K$ diagonal matrix with the vector $\mathbf{p}^{UL}$=$[p_1^{UL} \ldots p_k^{UL} \ldots p_K^{UL}]$ constituting the diagonal where p_i^{UL} is the average transmitted power of each user and $p_i^{UL} \geq 0$ for $i = 1, 2, \ldots, K$ and $\mathbf{z}$ is a vector of additive white Gaussian noise with zero mean. Without loss of generality the variance of $\mathbf{z}$ is considered to be 1 to reduce complexity.

For the detection of $\mathbf{x}$, the BS uses a $M \times K$ linear detector, $\mathbf{V}$ on $\mathbf{y}$ [5]. The signal and noise plus interference components of the processed received signal for the kth user after detection can thus be given as [5]
$$r_k = \underbrace{p_k^{UL}\mathbf{v}_k^H\mathbf{w}_k x_k}_{\text{desired signal}} + \underbrace{\sum_{i=1, i\neq k}^{K} p_i^{UL}\mathbf{v}_k^H\mathbf{w}_i x_i}_{\text{interference}} + \underbrace{\mathbf{v}_k^H\mathbf{n}}_{\text{noise}}, \quad (26)$$
where r_k and x_k are the kth elements of vectors $\mathbf{r}$ and $\mathbf{x}$ respectively while p_k^{UL} is the power transmitted by the kth user. We consider two low complexity detection schemes, namely MRC and ZF at the BS. Hence,
$$\mathbf{V} = \begin{cases} \mathbf{W}, & \text{for MRC} \\ \mathbf{W}\left(\mathbf{W}^H\mathbf{W}\right)^{-1}, & \text{for ZF.} \end{cases} \quad (27)$$
Assuming the channel to be ergodic, the ratio of the signal power of the kth user to the noise-plus-interference term (SINR) can be given as
$$\gamma_k^{UL} = \left(\frac{p_k^{UL}\,|\mathbf{v}_k^H\mathbf{w}_k|^2}{\sum_{i=1, i\neq k}^{K} p_i^{UL}|\mathbf{v}_k{}^H\mathbf{w}_i|^2 + \ ||\mathbf{v}_k||^2} \right). \quad (28)$$
Throughout this paper we assume the target SINR to be provided to each of the K users is equal. To achieve this equal SINR condition, we use the approach given in [26] for solving the power control problem in mobile scenarios using Perron's theorem[2]. Let us define a matrix $\mathbf{\Psi} \in \mathbb{C}^{K\times K}$, where
$$[\mathbf{\Psi}]_{k,i} = \begin{cases} \frac{|\mathbf{v}_k{}^H\mathbf{w}_i|^2}{\gamma_k^{UL}||\mathbf{v}_k||^2}, & \text{for } i \neq k \\ \frac{|\mathbf{v}_k{}^H\mathbf{w}_i|^2}{||\mathbf{v}_k||^2}, & \text{for } i = k. \end{cases} \quad (29)$$
Since, in our analysis the variance of $\mathbf{z}$ is considered to be 1, therefore, to meet the equal SINR condition for the K users, the uplink power vector $\mathbf{p}^{UL}$ has to satisfy the following condition [[26], eq. (29-33)]
$$\mathbf{p}^{UL}\mathbf{\Psi} = \mathbf{1}_{(1\times K)}. \quad (30)$$
Simplifying (29) and (30), the power assigned to each uplink user can be given as
$$p_k^{UL} = \frac{\gamma_k^{UL}}{q_k - \gamma_k^{UL}G_{ki}}, \quad (31)$$
where,
$$q_k = \frac{|\mathbf{v}_k{}^H\mathbf{w}_k|^2}{||\mathbf{v}_k||^2} \ \text{ and } \ G_{ki} = \begin{cases} \frac{|\mathbf{v}_k{}^H\mathbf{w}_i|^2}{||\mathbf{v}_k||^2}, & \text{for } i \neq k \\ 0, & \text{for } i = k. \end{cases} \quad (32)$$
The total transmitted power for K users during uplink can

[2]The model in [26] can be looked upon as a simplified generalization of our model without the mutual coupling effects. The power loss due to mutual coupling, p^{coup} in no way impacts the powers allocated to the users as this power loss is totally compensated for at the BS with additional circuitry. Moreover, any disparities in power distribution can also be accounted for by properly designing efficient detector or precoder matrices to meet the specific power constraints of the system.

now be given as

$$p_t^{UL} = E\{\mathbf{1}_{(1\times K)}\mathbf{p}^{UL}\}. \quad (33)$$

Remark 2. The power allocation problem states $p_k^{UL} > 0$. Hence, the necessary condition for p_k^{UL} to have a positive solution is that $q_k - \gamma_k G_{ki}$ be non-negative for $\gamma_k > 0$.

We now define the uplink SE for the kth user as [1]

$$R_k^{UL-A} = \left(\frac{T\Upsilon^{UL} - \tau^{UL}K}{T}\right)\tilde{R}_k^{UL-A}, \quad (34)$$

where $A \in \{MRC, ZF\}$, T is the coherence interval in symbols, τ^{UL} is the transmitted uplink pilot sequence and Υ^{UL} is the fraction of uplink transmission as described earlier.

Definition 1. Let a $p \times p$ matrix, $\mathbf{Q} \sim \mathcal{CW}_p(q, \mathbf{S})$, where p is the dimension, q is the degree of freedom and $\mathbf{S}$ is the covariance. Then from [27] for any integer $r > 0$,

1) $E\{\mathbf{Q}^r\} = \tilde{c}(r,q,p)\mathbf{S}$, where $\tilde{c}(r,q,p)$ is a constant depending on r, q, p. If $r = 1$, then $\tilde{c}(1,q,p) = q$. Hence, $E(\mathbf{Q}) = q\mathbf{S}$ and $E[tr(\mathbf{Q})] = pq\mathbf{S}$.
2) If $r = -1$, then $E(\mathbf{Q}^r) = \tilde{c}(1,q,p)\mathbf{S}^{-1}$ and $\tilde{c}(1,q,p) = (p-q)^{-1}$. Hence, $E(\mathbf{Q}^{-1}) = (p-q)^{-1}\mathbf{S}^{-1}$ and $E[tr(\mathbf{Q}^{-1})] = p(p-q)^{-1}\mathbf{S}^{-1}$.

Proposition 1. The first negative moment of the SINR for the kth user assuming $M \geq 2$, perfect CSI and MRC detection at the BS can then be given as

$$E\{(\gamma_k^{UL-MRC})^{-1}\} = \frac{Tr[\mathbf{\Sigma}_M^{-1}]\left(Tr[\mathbf{\Sigma}_M]\sum_{i=1,i\neq k}^{K} p_i^{UL}\beta_i + 1\right)}{p_k^{UL}(M-1)\beta_k}. \quad (35)$$

Accordingly, the uplink rate can be given as

$$\tilde{R}_k^{UL-MRC} = \log_2\left(1 + \left\{E\{(\gamma_k^{-1})^{UL-MRC}\}\right\}^{-1}\right) = \log_2\left(1 + \frac{p_k^{UL}(M-1)\beta_k}{Tr[\mathbf{\Sigma}_M^{-1}]\left(Tr[\mathbf{\Sigma}_M]\sum_{i=1,i\neq k}^{K} p_i^{UL}\beta_i + 1\right)}\right). \quad (36)$$

Now if $\tilde{\xi}_k$ is the minimum target SINR required to achieve a minimum rate of $\tilde{R}_k$ for the kth user, then the power required can be given as

$$= \frac{\tilde{p_k}^{UL-MRC}}{} \quad \frac{Tr[\mathbf{\Sigma}_M^{-1}]\tilde{\gamma_k}^{UL-MRC}}{(M-1)\beta_k - \tilde{\gamma_k}^{UL-MRC}Tr[\mathbf{\Sigma}_M]\sum_{i=1,i\neq k}^{K}\beta_i}. \quad (37)$$

Proof. See Appendix A. □

Proposition 2. The first negative moment of the SINR for the kth user assuming $M \geq K+1$, perfect CSI and ZF detection at the BS can thus be given as

$$E\{(\gamma_k^{UL-ZF})^{-1}\} = \frac{Tr[\mathbf{\Sigma}_M^{-1}]}{p_k(M-K)\beta_k}. \quad (38)$$

Accordingly, the uplink rate can be given as

$$\tilde{R}_k^{UL-ZF} = E\left[\log_2\left(1 + \left\{E\{(\gamma_k^{-1})^{UL-ZF}\}\right\}^{-1}\right)\right] = \log_2\left(1 + \frac{p_k^{UL}(M-K)\beta_k}{Tr[\mathbf{\Sigma}_M^{-1}]}\right). \quad (39)$$

If $\tilde{\gamma}_k$ is the minimum target SINR required to achieve a minimum rate of $\tilde{R}_k$ for the kth user, then the power required can be given as

$$\tilde{p_k}^{UL-ZF} = \frac{Tr[\mathbf{\Sigma}_M^{-1}]\tilde{\gamma_k}^{UL-ZF}}{(M-K)\beta_k}. \quad (40)$$

Proof. See Appendix B. □

B. Downlink

Since we use TDD transmission technique, the downlink channel can be represented as a Hermitian transpose of the uplink channel. The BS transmits data streams simultaneously to all the K users which creates an interfering broadcast channel. To encounter its effect we use a $M \times K$ precoding matrix at the BS denoted by $\mathbf{T}$. The signal received by the kth user can be given as

$$r_k = \underbrace{p_k^{DL} f \mathbf{w}_k^H \mathbf{t}_k x_k}_{\text{desired signal}} + \underbrace{\sum_{i=1,i\neq k}^{K} p_i^{DL} f \mathbf{w}_k^H \mathbf{t}_i x_i}_{\text{interference}} + \underbrace{z_k}_{\text{noise}}, \quad (41)$$

where $\mathbf{x} \in \mathbb{C}^{M\times 1}$ is the symbol transmitted by M antennas. $p_k^{DL} \subseteq \mathbf{p}^{DL} = [p_1^{DL} \dots p_k^{DL} \dots p_K^{DL}]^T$ is the power corresponding to the kth user similar to uplink with the same constraints while z_k is the noise associated with the kth user. $\mathbf{t}_k$ is the vector of the precodic matrix associated with the kth user and $f = \frac{1}{\sqrt{(\mathbf{T}\mathbf{T}^H)}}$ is a normalization parameter to constrain the average transmitted power. Almost identical to the case of uplink, we consider two linear precoding schemes namely MRT and ZF. Accordingly,

$$\mathbf{T} = \begin{cases} \mathbf{W}, & \text{for MRT} \\ \mathbf{W}\left(\mathbf{W}^H\mathbf{W}\right)^{-1}, & \text{for ZF.} \end{cases} \quad (42)$$

The desired SINR can thus be given as

$$\gamma_k^{DL} = \left(\frac{p_k^{DL}\frac{|\mathbf{w}_k^H\mathbf{t}_k|^2}{||\mathbf{t}_k||^2}}{\sum_{i=1,i\neq k}^{K} p_i^{DL}\frac{|\mathbf{w}_k{}^H\mathbf{t}_i|^2}{||\mathbf{t}_i||^2} + 1}\right). \quad (43)$$

Similar to uplink, we assume the target SINR to be provided to each of the K users is equal. Following the same approach as used to derive (31), the downlink power for the kth user can be assigned as

$$p_k{}^{DL} = \frac{\gamma_k^{DL}}{q_k - \gamma_k G_{ki}}, \quad (44)$$

where

$$q_k = \frac{|\mathbf{w}_k{}^H\mathbf{t}_k|^2}{||\mathbf{t}_k||^2} \text{ and } G_{ki} = \begin{cases} \frac{|\mathbf{w}_k{}^H\mathbf{t}_i|^2}{||\mathbf{t}_k||^2}, & \text{for } i \neq k \\ 0, & \text{for } i = k. \end{cases} \quad (45)$$

The total transmitted power for K users during downlink can now be given as

$$p_t^{DL} = E\{\mathbf{1}_{(1\times K)}\mathbf{p}^{DL}\}. \tag{46}$$

Remark 3. Adhering to the power constraint $p_k^{DL} > 0$, the necessary condition for p_k^{DL} to have a positive solution is that $q_k - {\gamma^{DL}}_k G_{ki}$ be non-negative for $\gamma_k^{DL} > 0$.

The downlink rate similar to the uplink for the kth user can now be given as

$$R_k^{DL-A} = \left(\frac{T\Upsilon^{DL} - \tau^{DL}}{T}\right)\tilde{R}_k^{DL-A}, \tag{47}$$

where $A \in \{MRC, ZF\}$, T is the coherence interval in symbols, τ^{DL} is the transmitted downlink pilot sequence and Υ^{DL} is the fraction of downlink transmission as described earlier.

Proposition 3. With $M \geq 2$ and assuming perfect CSI and MRC detection at the BS, the first negative moment of the SINR for the kth user can be given as

$$E\{(\gamma_k^{DL-MRC})^{-1}\} = \frac{Tr[\mathbf{\Sigma}_M^{-1}]\left(Tr[\mathbf{\Sigma}_M]\sum_{i=1,i\neq k}^{K} p_i^{DL}\beta_i + 1\right)}{p_k^{DL}(M-1)\beta_k}. \tag{48}$$

The downlink rate, $\tilde{R}_k^{DL-MRC}$ follows accordingly similar to proposition 1. Also if $\tilde{\gamma}_k$ is the minimum target SINR required to achieve a minimum rate of $\tilde{R}_k$, then the power required can be given as

$$\tilde{p_k}^{DL-MRC} = \frac{Tr[\mathbf{\Sigma}_M^{-1}]\tilde{\gamma_k}^{DL-MRC}}{(M-1)\beta_k - \tilde{\gamma_k}^{DL-MRC}Tr[\mathbf{\Sigma}_M]\sum\limits_{i=1,i\neq k}^{K}\beta_i}. \tag{49}$$

Proof. Following the same derivations as in proposition 1 for the case of uplink, we can arrive at the above result. □

Proposition 4. With $M \geq K+1$ and assuming perfect CSI and ZF detection at the BS, the first negative moment of the SINR for the kth user is given as

$$E\{(\gamma_k^{DL-ZF})^{-1}\} = \frac{Tr[\mathbf{\Sigma}_M^{-1}]}{p_k^{DL}(M-K)\beta_k}. \tag{50}$$

The downlink rate, $\tilde{R}_k^{DL-ZF}$ follows accordingly similar to proposition 2. Accordingly, if $\tilde{\gamma}_k$ is the minimum target SINR required to achieve a minimum rate of $\tilde{R}_k$, then the power required can be given as

$$\tilde{p_k}^{DL-ZF} = \frac{Tr[\mathbf{\Sigma}_M^{-1}]\tilde{\gamma_k}^{DL-ZF}}{(M-K)\beta_k}. \tag{51}$$

Proof. This proof can be obtained following a similar approach as to the derivation of proposition 2 for the case of uplink. □

IV. Energy Efficiency

EE of a communication link as stated in Section I is the total transmit energy consumption required per bit i.e., ratio of the sum rate achieved to the consumed power, and can be expressed in bits/joule as [1], [7], [21], [31], [32], [35][3].

$$\xi^A = \frac{R^A}{p^{PA} + p^{RF} + p^{Coup}}, \tag{52}$$

where $R^A = \sum\limits_{k=1}^{K}(R_k^{UL-A} + R_k^{DL-A})$ is the total sum rate for the K users through an entire process of uplink and downlink, p^{PA} is the power consumed by the power amplifiers, p^{RF} is the power consumed by the RF components of the systems, p^{Coup} is the power loss due to mutual coupling among the antennas located in close proximity of each other and $A \in \{MRC, ZF\}$.

Remark 4. In order to obtain insights on how the number of antennas, the physical space and the transmitted power affect the total EE of a massive MIMO system, it makes sense to look at the total rate and divide it by the total power. Hence, the EE metric used in this paper focuses on the total rate and power of both uplink and downlink. Following [7], [31], [32], we look at the system as a whole, but with the important discrepancy that the increase in the number of BS antennas happens in a fixed physical space.

A. Power Amplifiers

The average power in watt consumed by the power amplifiers during uplink and downlink can be approximated as [21], [7]

$$p^{PA} = p_t^{UL}(\alpha^{UL} + 1) + p_t^{DL}(\alpha^{DL} + 1), \tag{53}$$

where $\alpha^{UL} = \frac{\zeta^{UL}}{\eta^{UL}} - 1$ and $\alpha^{DL} = \frac{\zeta^{DL}}{\eta^{DL}} - 1$ with ζ^{UL} and ζ^{DL} being the modulation-dependent peak to average power ratios (PAPR) for uplink and downlink respectively while η^{UL} and η^{DL} are the power amplifier efficiencies at the UD and BS respectively and p_t^{UL}, p_t^{DL} are the transmitted powers in the uplink and downlink respectively as described earlier. It is to be noted that the total PAPR for UL and DL is equal to 1.

B. RF Chains

The average power in watt consumed in the RF chains for a typical MIMO transmitter-receiver set can be given as [21]

$$p^{RF} = p_{fix}^A + Mp^{BS} + Kp^{UE} \tag{54}$$

where p_{fix}^A is the fixed power consumption at the BS dependent on the processing scheme $A \in \{MRC, ZF\}$, p^{BS} is the

[3]The definition of EE used in this paper is in accordance with the mentioned literatures. This approach of dividing the SE with the average total power consumption greatly simplifies the analysis and is comparable to the various recent literature on MIMO systems. The joint uplink-downlink optimization makes it favorable to attain a a holistic and balanced optimization for the uplink and downlink resources, system parameters (such as antenna numbers) and to allow a performance guarantee vs power consumption on the full forward and reverse link between the base station (BS) and mobile users [38], [39], [40].

power required at the BS to run the circuit components, p^{UE} is the power associated with the user equipments which are defined as follows

$$p^{BS} = p^{BS}_{mix} + p^{BS}_{filt} + p^{BS}_{ADC} + p^{BS}_{DAC} + p^{BS}_{OSC}, \quad (55)$$

$$p^{UE} = p^{UE}_{mix} + p^{UE}_{filt} + p^{UE}_{ADC} + p^{UE}_{DAC} + p^{UE}_{OSC}, \quad (56)$$

where p_{mix}, p_{filt}, p_{ADC}, p_{DAC} and p_{OSC} denote the power consumed by the mixers, filters, analog-to-digital converters, digital-to-analog converters and local oscillator respectively[4].

C. Mutual Coupling

The mutual coupling effect among antennas in the vicinity of each other as discussed earlier increases the power consumption of the system. Applying simple circuit theory analysis on Fig. 2, the terminal voltage for a particular antenna at the BS can be given as [10]

$$\mathrm{v}_i = \sum_{j=1, i\neq j}^{M} \mathrm{i}_j \Gamma_{i,j}, \quad (57)$$

where, v_i denotes the terminal voltage at the ith antenna element due to a unity current in the jth antenna element when the current in all other antenna elements is zero and $\Gamma_{i,j}$ is the total mutual coupling experienced by the ith antenna element due to all other antennas as discussed in section III. Furthermore, $\mathbf{i}_{BS} = [\mathrm{i}_1, \mathrm{i}_2, \mathrm{i}_3 \ldots\ldots \mathrm{i}_M]^T$, and $\mathbf{v}_{BS} = [\mathrm{v}_1, \mathrm{v}_2, \mathrm{v}_3 \ldots\ldots \mathrm{v}_M]^T$ where, $\mathbf{i}_{BS}$ and $\mathbf{v}_{BS}$ are vectors of currents and voltages respectively associated with the dipole antennas in the rectangular array. The power loss due to coupling based on the current maximum now follows as

$$p^{coup} = \mathbf{v}^T_{\mathrm{BS}} \mathbf{i}_{\mathrm{BS}}. \quad (58)$$

In order to maintain a fixed SINR, this loss is compensated at the BS. Using (52)-(58) we now derive an analytical expression for ξ. For the sake of simplicity, we consider the minimum SINR, γ targeted for every users to be equal for both uplink and downlink.

Hereinafter, we consider a minimum fixed rate, $\tilde{R}$ to be provided to each and every user for both uplink and downlink which leads to the uplink and downlink rates being $\Upsilon^{UL}\tilde{R}$ and $\Upsilon^{DL}\tilde{R}$ respectively. Thus the total SE of the system for one complete cycle of uplink and downlink can be given as

$$\begin{aligned} R^A &= \sum_{k=1}^{K} \left[\left(\frac{T\Upsilon^{UL} - K\tau^{UL}}{T} \right) \tilde{R}^{UL-A}_k \right. \\ &\quad \left. + \left(\frac{T\Upsilon^{DL} - K\tau^{DL}}{T} \right) \tilde{R}^{DL-A}_k \right] \\ &= \frac{K\tilde{R}}{T} \left[T - K(\tau^{UL} + \tau^{DL}) \right]. \end{aligned} \quad (59)$$

[4]The components considered in this paper may vary depending on set-ups used in practical scenarios. Any other components used can easily be included in the expressions of p^{BS} and p^{UE} while the ones that are not may be removed. It is to be noted that the uplink and downlink transmissions are separated by the fractions Υ^{UL} and Υ^{DL} respectively. Hence, by changing these parameters, the uplink and downlink power consumption parameters can be controlled to adjust to the requirement of the networks in consideration.

Proposition 5. Taking into account the diversity loss due to mutual coupling, we aim at guaranteeing a minimum rate of $\tilde{R}$. We accomplish this by dynamically allocating power to the users and hence, define a parameter $\bar{p} = f(\gamma, \tilde{R})$. Therefore, considering ZF processing at the BS, with no loss of generality, we can define $\tilde{R}$ as

$$\tilde{R} = \log_2(1 + \bar{p}(M - K)). \quad (60)$$

Thus the total power consumed by the power amplifiers during one complete cycle of uplink and downlink when a ZF processing scheme is employed at the BS is

$$p^{PA}_{ZF} = K\bar{p}\, Tr[\mathbf{\Sigma}^{-1}_M] \left(\frac{\zeta^{UL}}{\eta^{UL}} + \frac{\zeta^{DL}}{\eta^{DL}} \right). \quad (61)$$

Proof. See Appendix C. □

D. Energy Efficiency and Analytical Optimum of M for ZF

The EE of the system now follows from (50) on top of the following page as (62), where p^{BS}, p^{UE}, and p^{Coup} are obtained from (53), (54) and (58) respectively.

Definition 2. If a local maximum exists in a strictly quasi-concave function, it is also the global maximum [37]. This global optimum can then be obtained by setting the partial derivative of the quasi-concave function to zero.

Proposition 6. Considering ZF processing scheme at BS and diversity loss due to mutual coupling, the maximum number of antennas, M that can be accommodated within a fixed physical space, Δ which maximizes the EE, ξ^{ZF} can be given on top of the following page as (63), where $W(*)$ is the product logarithm function and $e = 2.71828$ is the Euler's number. The rest of the parameters have already been discussed before.

Proof. See Appendix D. □

Furthermore, it can also be shown that the stationary point M_{max} is also a global maximum and the EE curve is quasi-concave, which increases for $K + 1 \leq M \leq M_{max}$, attains a global maximum, M_{max} and then decreases for $M_{max} \leq M \leq \infty$ (See Appendix D).

At this point it is worth mentioning the relation between $\mathbf{\Sigma}_M$ and M. While there is no explicit mathematical expression relating these two parameters directly, from (15) it can be seen that $\mathbf{\Sigma}_M$ is related to Γ, which in turn is related to Z through (13-16). However, Z depends on m, n and the distance d through (17-22). Since the physical space Δ of the antenna array is constant, any changes made on M will affect the mutual coupling Z and subsequently the resulting correlation $\mathbf{\Sigma}_M$, which is indeed intuitive.

Proposition 7. Considering ZF processing scheme at BS and diversity loss due to mutual coupling, the parameter $\bar{p}$ that maximizes the EE, ξ^{ZF} provided M is kept constant can be given on top of the following page as (64).

Proof. See Appendix E. □

$$\xi^{ZF} = \frac{\frac{K}{T}\left(T - K(\tau^{UL}\tau^{DL})\right)\log_2(1+\bar{p}(M-K))}{K\bar{p}\,Tr[\mathbf{\Sigma}_M^{-1}]\left(\frac{\zeta^{UL}}{\eta^{UL}} + \frac{\zeta^{DL}}{\eta^{DL}}\right) + Mp^{BS} + Kp^{UE} + p^{Coup}} \tag{62}$$

$$M_{max} = \frac{1}{\bar{p}}\left[\exp\left\{W\left(\frac{\bar{p}\left(K\bar{p}\,Tr[\mathbf{\Sigma}_M^{-1}]\left(\frac{\zeta^{UL}}{\eta^{UL}} + \frac{\zeta^{DL}}{\eta^{DL}}\right) + Kp^{UE} + p^{Coup}\right)}{p^{BS}e} - \frac{1-\bar{p}K}{e}\right) + 1\right\} + \bar{p}K - 1\right] \tag{63}$$

$$\bar{p}_{max} = \frac{1}{M-K}\left[\exp\left\{W\left(\frac{(M-K)(Mp^{BS} + Kp^{UE} + p^{Coup})}{K\,Tr[\mathbf{\Sigma}_M^{-1}]\left(\frac{\zeta^{UL}}{\eta^{UL}} + \frac{\zeta^{DL}}{\eta^{DL}}\right)e} - \frac{1}{e}\right) + 1\right\} - 1\right] \tag{64}$$

V. Results and Discussion

On the basis of the proposed system model for massive MIMO, we analyze the effect of mutual coupling and correlation on the SE and EE of massive MIMO systems through Monte Carlo simulations with respect to M, Δ and d, which is calculated as explained in Example 1. We also test the validity of these results with analytical proofs. As mentioned earlier, the fixed power consumption for two current technologies namely WIFI and LTE are considered to obtain a fair comparison.

We consider a single hexagonal cell with a diameter of $s_{max} = 3000$ meters which extends from vertex to vertex. The BS is located at the center of the cell with $K = 10$ users uniformly distributed in the cell. The minimum distance, s_{min} between a user and the BS is 50 meters. The large scale fading as described in the system model is defined as $\beta_k = \frac{t_k}{(s_k/s_{min})^{\nu}}$, where t_k is the log-normal random variable with a variance σ_s^2, s_k is the distance between the kth user and the BS varying anywhere between s_{min} and s_{max} and ν is the path-loss exponent varying from 2 to 4 with 2 denoting free space propagation and 4 denoting a relatively lossy environment. For our simulations we choose $\sigma_s = 10dB$ and $\nu = 3.8$. In the above channel model, unless stated otherwise, a fixed total physical space is assumed with the dimensions (length:width) of the rectangular array following a fixed ratio of $\alpha : \beta = 1 : 1$. In other words, we consider a square array with equal number of antennas along the length and the width of the array. This ratio is just for our analytical tractability and can be modified according to the requirements of the set-up. Furthermore, the area of this space is limited to $\alpha\beta\lambda^2$, where λ is the carrier wavelength. To simplify the V-I characteristics calculations, the antenna elements are considered to be simple dipoles. The length of all the M dipoles are considered to be 0.5λ. All the simulation parameters used are given on top of the following page in Table I. We adhere to the 3GPP standards and unless mentioned otherwise most of the values of the parameters used are inspired from the literature mentioned in the references [2], [7], [8], [36].

A. Traditional model- Antenna spacing greater than half the carrier wavelength :

To comprehend the effects of constrained physical spaces in a massive MIMO set-up, we first analyze its performance based on a system model where the spacing among the antennas is considered to be greater than half the carrier wavelength; thus negating any effects of mutual coupling. For this case we can consider $\mathbf{Z}$ as an all-ones matrix. This model will allow us to analyze the dependency of the correlation on d and also lay a platform for our analysis of mutual coupling later. The curves in Fig. 4 labeled as 'without coupling' illustrate this scenario.

B. Proposed model- Antenna spacing less than half the carrier wavelength :

In this sub-section we analyze the behaviour of the proposed model by increasing the number of antennas at the BS while keeping the area of the rectangular array fixed. Typically for a fixed physical spacing, increasing the number of antennas is associated with decreasing the antenna spacing; thus increasing mutual coupling which in turn reduces the EE. Therefore, there is a fundamental trade-off between the EE of the system and the number of antennas at the BS, which will be evident from the simulation results.

Fig. 3 illustrates the SE of the proposed system with a fixed physical space and shows its variation as a function of M. The spacing among the antennas varies depending on the number of antennas which in turn affects the mutual coupling matrix. Here we show the achievable SE in a massive MIMO system with coupling, considering MRC/MRT and ZF detection and precoding at the BS. The length and width of the array are constrained as $\alpha = 5$ and $\beta = 5$ which is kept fixed hereinafter unless stated otherwise. We increment the total number of antennas in squares. For example, $n = 1, 3, 5, \ldots$ and $m = 1, 3, 5, \ldots$ which implies $M = 1, 9, 25, \ldots$ where n and m are the number of antennas along the width and length respectively of the array. As expected with the increase in M, the SE of the system also increases. We note however, that the improvement in SE saturates for high numbers of antennas due to the significant correlation and coupling. For the same reason ZF outperforms MRC by a large extent. Also it can be seen that systems corresponding to LTE systems with a higher fixed transmission power offer higher SE as compared to WIFI systems with a lower fixed transmission power. For the case of ZF the difference in throughput for the two power schemes is higher than for the case of MRC where the gap between their respective performance is much less. We next specifically examine the EE of such a system in detail. In Fig. 4, we consider two settings: one where the physical space is

TABLE I: Simulation Parameters

Parameter	Value	Parameter	Value
Length of coherence interval, T	196	Length of the dipoles, l	0.5λ
Fraction of UL Transmission,Υ^{UL}	0.4	PAPR uplink, ζ^{UL}	0.4
Fraction of DL Transmission,Υ^{DL}	0.6	PAPR downlink, ζ^{DL}	0.6
Channel coherence time, T_c	1 ms	PA efficiency BS, η^{DL}	0.39
Length of pilots, τ^{UL}, τ^{DL}	10	PA efficiency UE, η^{UL}	0.3
Array length, $\alpha\lambda$	5λ	p_{fix}^{WIFI}	25dBm
Array width, $\beta\lambda$	5λ	p_{fix}^{LTE}	43dBm
Antenna impedance, Z_A	50Ω	p_{OSC}^{BS}	33dBm
Load impedance, Z_L	50Ω	p_{OSC}^{UE}	17dBm
Length:Width ratio of array, $\alpha:\beta$	1:1	$p_{mix}^{BS}+p_{filt}^{BS}+p_{DAC}^{BS}+p_{DAC}^{BS}$	30dBm
Number of DODs/DOAs, D	150	$p_{mix}^{UE}+p_{filt}^{UE}+p_{DAC}^{UE}+p_{DAC}^{UE}$	16.9dBm

not bounded by any limitations while for the other, a similar setting to Fig. 3 is considered. For the first setting, the antennas are spaced far apart to negate any effects of coupling. This figure provides insights into EE of massive MIMO systems with and without coupling with MRC detection/precoding. We plot the EE with respect to the number of BS antennas M. The dashed lines show the performances of WIFI systems while the continuous line represents LTE systems like before. Now as d is inversely proportional to M, it decreases with increasing M; thus also decreasing EE which is evident from the curve. For example, for $M = 100$ the EE falls from 4.8 Kbits/J (without coupling) to 2.7 Kbits/J when coupling is considered. Also to be noted is the shape of the EE curve. As stated in proposition 6, the EE curve considering coupling is seen to be concave. However, the EE curve without coupling is also seen to be concave which eventually decreases with increasing M. This is due to the more accurate power consumption model we have used in the paper, which is further exacerbated by the increasing correlation between the antennas. For example, each antenna at the BS has its individual circuitry, which has non-zero power consumption and hence the power consumed by the BS is a multiple of the number of antennas, M. Most existing works consider p^{BS} to be constant and accordingly when M goes to infinity, the EE becomes unbounded. Our results on the contrary show that when the power at the BS is equal to Mp^{BS} the EE does not always increase and is a concave function of M. Furthermore, when coupling is not considered, p_k^{RF} in (52) still holds with ξ^{ZF} in (60) staying the same but without the mutual coupling term, $Tr[\mathbf{\Sigma}_M^{-1}]$ which can be shown to be concave similar to what was shown in proposition 6.

Moreover, WIFI systems with low power consumption naturally perform better from EE point of view like before but when coupling is considered the gap in their performances reduces with the increase in the number of antennas, M. Furthermore, depending on the system model and channel detection/ precoding technique used, it is a concave or quasi-concave function of M.

Hereinafter, we consider three scenarios with three different physical spaces: a) $\Delta = 3\lambda \times 3\lambda$, b) $\Delta = 5\lambda \times 5\lambda$, c) $\Delta = 7\lambda \times 7\lambda$. Fig. 5 considers scenario (a) and compares

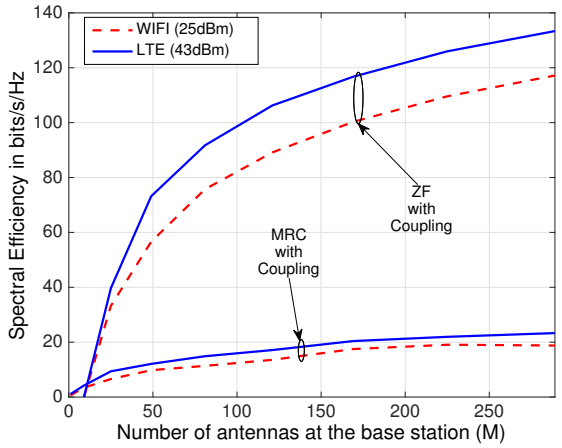

Fig. 3: Spectral Efficiency with respect to M using MRC/MRT and ZF detection/precoding at the BS for two fixed power consumption schemes. In this example, $\alpha = 5$ and $\beta = 5$.

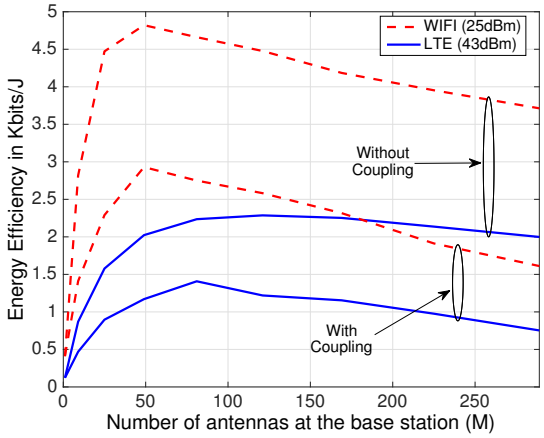

Fig. 4: Energy Efficiency with respect to M with and without coupling at the BS using MRC detection/ precoding at the BS for two fixed power consumption schemes. In this example, $\alpha = 5$ and $\beta = 5$.

the performances of MRC/MRT and ZF with respect to EE considering mutual coupling at the BS. The settings are kept

This article has been accepted for publication in a future issue of this journal, but has not been fully edited. Content may change prior to final publication. Citation information: DOI 10.1109/TWC.2016.2522419, IEEE Transactions on Wireless Communications

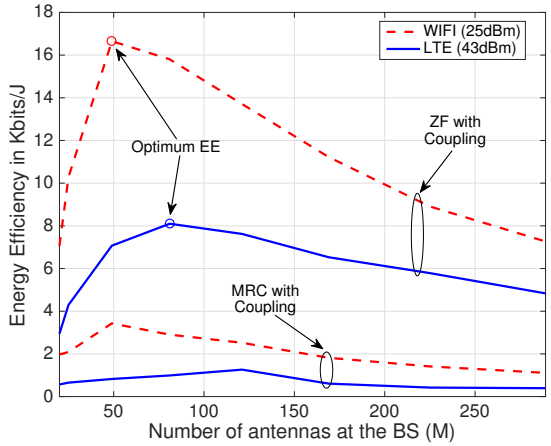

Fig. 5: Energy Efficiency with respect to M with coupling at the BS using MRC and ZF detection/ precoding at the BS for two fixed power consumption schemes. In this example, $\alpha = 3$ and $\beta = 3$.

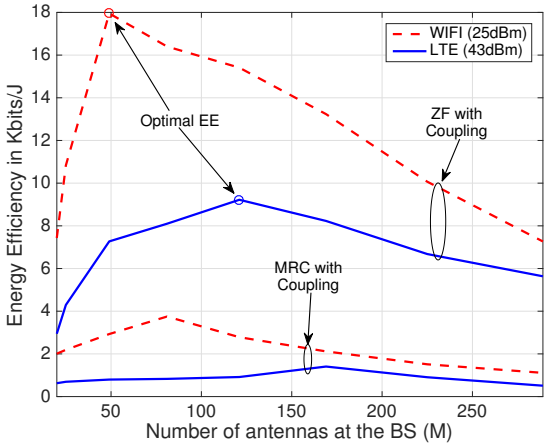

Fig. 6: Energy Efficiency with respect to M with coupling at the BS using MRC and ZF detection/ precoding at the BS for two fixed power consumption schemes. In this example, $\alpha = 5$ and $\beta = 5$.

exactly same as Fig. 3 except for Δ. ZF outperforms MRC for both the cases of WIFI and LTE as ZF is seen to give at least five times more throughput than MRC. Similar to Fig. 4, the performance gap between WIFI and LTE systems reduces for both ZF and MRC. The optimal M for ZF as calculated in section V is also plotted. The figure shows that for WIFI systems 49 antennas and for LTE systems 81 antennas give a global optimum EE.

Fig. 6 considers scenario (b) while Fig. 7 scenario (c). The rest of the settings are kept exactly the same as Fig. 3. The results are similar to Fig. 5 as can be expected. The EE performance can be seen to improve due to the relaxation in BS physical area. However, it is to be noted that the optimal M changes as the dimensions of D increase. The optimality shifts towards the right as we increase the physical space. With a spacing of $\Delta = 5\lambda \times 5\lambda$, M for WIFI and LTE systems to give a global EE are 49 and 121 respectively while for $\Delta = 7\lambda \times 7\lambda$, M is 81 and 121 for WIFI and LTE systems respectively. This is due to the changes in $\bar{p}_{max}$ owing to the effects of mutual coupling which accounts for M_{max}. This can be considered a trade-off between the number of antennas, M, the fixed physical space, Δ and EE.

At this point, we would like to further stress on the fact that there is a trade-off between the EE and SE of the system. This trade-off is in line with [1] and [30], where similar results were obtained but with different system models. Due to the consideration of the circuit power consumption at the BS which is a function of M, though the SE increases asymptotically, the EE does not. To explicitly show this trade-off, Fig. 8 considers the scenario with the bounded dimension of $\Delta = 5\lambda \times 5\lambda$. It can be seen from the figure that as the SE of the system increases, the EE of the system increases to an extent and then starts to fall sharply. From (64) it is implicit that EE is a quasi concave function of the parameter $\bar{p}$. Additionally, $\bar{p}_{max}$ in (64) can be looked upon as the optimum power required to attain the maximum EE for a

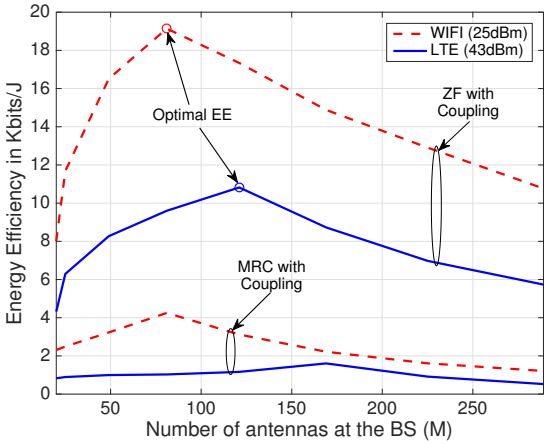

Fig. 7: Energy Efficiency with respect to M with coupling at the BS using MRC and ZF detection/ precoding at the BS for two fixed power consumption schemes. In this example, $\alpha = 7$ and $\beta = 7$.

certain antenna array dimension. The SE on the other hand is a monotonically increasing function of $\bar{p}$ as can be seen from (58). This explains the quasi concavity of the of the plot between SE and EE. Furthermore, following the course of the previous figures, WIFI systems show better performance than their LTE counterparts with respect to EE. $\bar{p}$ can be of paramount importance to network engineers while deciding on operating regimes where it is possible to jointly increase the SE and EE of the system. For other regimes however, $\bar{p}$ can be set according to the current traffic demands, for e.g., during night time when the traffic is low, $\bar{p}$ can be set to achieve high EE with a constraint on the SE.

Fig. 9 shows the impact of the number of antennas, M on the power loss due to coupling at the BS for different antenna spacings. Though the power loss due to coupling has already

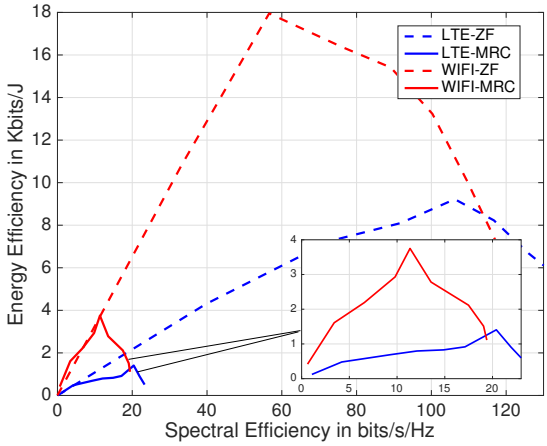

Fig. 8: An illustration of the trade-off between energy efficiency and spectral efficiency. In this example, $\alpha = 5$ and $\beta = 5$.

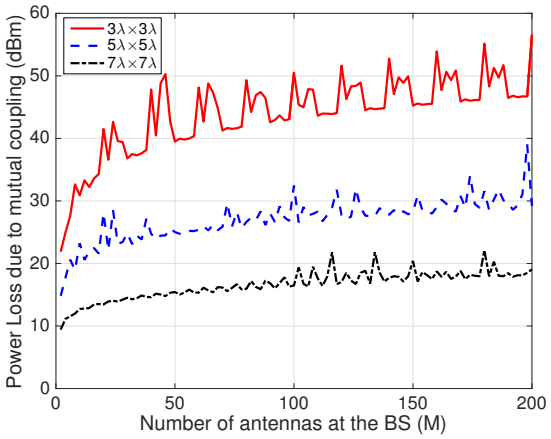

Fig. 9: Power loss due to mutual coupling with respect to M considering different array dimensions.

been taken into consideration in the previous results and figures, this figure specifically explains the variation of power loss due to mutual coupling. The settings are kept similar to Fig. 3. It can be seen from the figure that as the spacing between antennas is reduced, mutual coupling increases and so does the power loss due to coupling. The large variation between the $3\lambda \times 3\lambda$ and the other two curves is due to more compact physical spacing among the antennas, which results in more loss due to mutual coupling. As stated before, we aim at restricting the physical space to within $1m^2$. Hence, for example, considering about 100 antennas for the case of $3\lambda \times 3\lambda$ scenario, the spacing between any two adjacent antennas is equal to $0.1m$, which is less than half the wavelength of a 900 MHz GSM band and this introduces increasing amount of mutual coupling with increasing numbers of antennas. The constructive and destructive superposition of the signals due to mutual coupling is periodic with this decrease in separation for a fixed wavelength, which contributes to the periodic behavior of the power loss.

VI. Conclusion

Conventionally, massive MIMO systems are considered to achieve high EE with the increase in number of BS antennas which might be misleading when antenna coupling along with circuit power consumptions are considered. We have given an analysis of the effects of mutual coupling on the EE for realistic massive MIMO systems. Simulation results show that as the spacing between the antennas is reduced, the coupling among them increases, resulting in a dip in EE performance. We also reveal that the EE is a decreasing concave or quasi-concave function of M. A trade-off between the number of antennas, M, the fixed physical space, Δ and EE is found. Depending on the physical space, optimum number of antennas are found with the objective of achieving high EE. It is evident that high EE can be obtained but at the cost of reducing M or increasing Δ.

Appendix A
Proof of Proposition 1

For MRC, $\gamma_k^{UL-MRC} = \left(\frac{p_k^{UL} ||\mathbf{w}_k||^4}{\sum_{i=1,i\neq k}^{K} p_i^{UL} |\mathbf{w}_k{}^H \mathbf{w}_i|^2 + ||\mathbf{w}_k||^2} \right)$.

Dividing both the numerator and denominator by $||\mathbf{w}_k||^2$ and defining $\bar{w}_i = \frac{\mathbf{w}_k{}^H \mathbf{w}_i}{||\mathbf{w}_k||}$, where $\bar{w}$ is a Gaussian random variable with variance $Tr(\mathbf{\Sigma}_M)\beta_i$, we have

$$E\{(\gamma_k^{UL-MRC})^{-1}\} = \left(\sum_{i=1,i\neq k}^{K} p_i^{UL} E\{|\bar{w}_i|^2\} + 1 \right) E\left(\frac{1}{p_k^{UL} ||\mathbf{w}_k||^2} \right). \quad (65)$$

Now using the property $||\mathbf{A}|| = \sqrt{Tr(\mathbf{A}^H \mathbf{A})}$ and definition 1, we have

$$E\{(\gamma_k^{UL-MRC})^{-1}\} = \left(Tr(\mathbf{\Sigma}_M) \sum_{i=1,i\neq k}^{K} p_i^{UL} \beta_i + 1 \right) \frac{Tr\left[\mathbf{\Sigma}_M^{-1}\right]}{p_k^{UL}(M-1)\beta_k}. \quad (66)$$

Following a similar approach on (33), we obtain (37).

Appendix B
Proof of Proposition 2

For ZF, $\gamma_k^{UL-ZF} = \frac{p_k^{UL}}{[(\mathbf{W}^H\mathbf{W})^{-1}]_{kk}}$. Hence

$$\begin{aligned} E\left\{ \left[(\mathbf{W}^H\mathbf{W})^{-1} \right]_{kk} \right\} &= \frac{1}{K\beta_k} E\left\{ Tr\left[(\mathbf{W}^H\mathbf{W})^{-1} \right] \right\} \\ &= \frac{Tr\left[\mathbf{\Sigma}_M^{-1}\right]}{p_k^{UL}(M-K)\beta_k}, \end{aligned} \quad (67)$$

which is obtained by using definition 1. Now from (33) and (38) we obtain (40).

Appendix C
Proof of Proposition 5

For ZF, $\gamma_k^{UL-ZF} = \frac{p_k^{UL}}{[(\mathbf{W}^H\mathbf{W})^{-1}]_{kk}}$. Hence, from (60) we have, $p_k^{ZF} = \bar{p}(M-K)\left[(\mathbf{W}^H\mathbf{W})^{-1}\right]_{kk}$. Therefore, using

definition 1 and from (40), (51) and (53) we have

$$\begin{aligned} p_{ZF}^{PA} &= K\bar{p}(M-K)\left(\frac{\zeta^{UL}}{\eta^{UL}}+\frac{\zeta^{DL}}{\eta^{DL}}\right)E\left\{Tr\left[(\mathbf{W}^H\mathbf{W})^{-1}\right]\right\} \\ &= K\bar{p}(M-K)\left(\frac{\zeta^{UL}}{\eta^{UL}}+\frac{\zeta^{DL}}{\eta^{DL}}\right)\frac{Tr\left[\mathbf{\Sigma}_M^{-1}\right]}{M-K} \\ &= K\bar{p}Tr[\mathbf{\Sigma}_M^{-1}]\left(\frac{\zeta^{UL}}{\eta^{UL}}+\frac{\zeta^{DL}}{\eta^{DL}}\right). \end{aligned} \tag{68}$$

APPENDIX D
PROOF OF PROPOSITION 6

We rewrite (62) as

$$\xi^{ZF}(M)=\frac{\frac{K}{T}\left(T-K(\tau^{UL}\tau^{DL})\right)\log_2(1-\bar{p}K+\bar{p}M)}{K\bar{p}Tr[\mathbf{\Sigma}_M^{-1}]\left(\frac{\zeta^{UL}}{\eta^{UL}}+\frac{\zeta^{DL}}{\eta^{DL}}\right)+Kp^{UE}+p^{Coup}+Mp^{BS}}. \tag{69}$$

Let $(1-\bar{p}K)=a$, $\bar{p}=b$, $K\bar{p}Tr[\mathbf{\Sigma}_M^{-1}]\left(\frac{\zeta^{UL}}{\eta^{UL}}+\frac{\zeta^{DL}}{\eta^{DL}}\right)+Kp^{UE}+p^{Coup}=c$, $p^{BS}=d$ and $\frac{K}{T}\left(T-K(\tau^{UL}\tau^{DL})\right)=f$. Therefore, (69) implies

$$\xi^{ZF}(M) = \frac{f\log_2(a+bM)}{c+dM}. \tag{70}$$

In order to prove that the objective function, $\xi^{ZF}(M)$ is quasi-concave it is sufficient to prove that the upper contour sets $S_\psi=\{M\succeq 0|\xi^{ZF}(M)\geq\psi\}$ of $\xi^{ZF}(M)$ are convex for any $\psi\in\mathbb{R}$ [34]. We investigate the cases when $\psi\leq 0$ and $\psi>0$. When $\psi\leq 0$, the set is empty in the contour $\xi^{ZF}(M)=\psi$. Thus $\xi^{ZF}(M)$ is strictly quasi-convex when $\psi\leq 0$. Now when $\psi>0$, S_ψ is equivalent to

$$\begin{aligned} &\left\{M\geq 0\,\middle|\,\frac{f\log_2(a+bM)}{c+dM}\geq\psi\right\} \\ \Longrightarrow\quad &\left\{M\geq 0\,\middle|\,c\psi+dM\psi-f\log_2(a+bM)\leq 0\right\}. \end{aligned}$$

Let $F=c\psi+dM\psi-f\log_2(a+bM)$. Now, F is strictly convex within the range of M as its Hessian is positive definite. Hence, S_ψ is strictly convex, which concludes that $\xi^{ZF}(M)$ is a quasi-concave function of M.

Now using Definition 2, we can say that the local maximum of ξ^{ZF} is also the global maximum. Furthermore, as $M\to\infty$, $\xi^{ZF}\to 0$. Since $M\not\leq 0$, the local maximum is obtained by calculating the first derivative and setting it to zero as shown below. From (70) we have

$$\begin{aligned} \frac{\partial\xi^{ZF}(M)}{\partial M} &= \frac{\partial\left(\frac{f\log_2(a+bM)}{c+dM}\right)}{\partial M} \\ &= \frac{fb}{(a+bM)(c+dM)\ln 2}-\frac{fd\ln(a+bM)}{(c+dM)^2\ln 2}. \end{aligned} \tag{71}$$

Now equating the right hand side of (71) to zero, we have

$$\begin{aligned} \frac{b(c+dM)}{a+bM} &= d\ln(a+bM) \\ \Longrightarrow \frac{bc-ad}{a+bM} &= d\left(\ln(a+bM)-1\right). \end{aligned} \tag{72}$$

Let $\ln(a+bM)-1=x$. Therefore $\exp(x+1)=a+bM$. Thus (72) implies

$$\begin{aligned} \frac{bc-ad}{\exp(x+1)} &= dx \\ \Longrightarrow \frac{bc}{de}-\frac{a}{e} &= x\exp(x) \\ \Longrightarrow x &= W\left(\frac{bc}{de}-\frac{a}{e}\right), \end{aligned} \tag{73}$$

where W, known as the product logarithm is the inverse function of $f(W)=We^W$ for any complex number W. Substituting x with $\ln(a+bM)-1$ we have

$$M_{max}=\frac{\exp\left\{W\left(\frac{bc}{de}-\frac{a}{e}\right)+1\right\}-a}{b}. \tag{74}$$

Now replacing a,b,c,d with their equivalent parameters, we obtain (63). Quasi-concavity thus implies that M_{max} is a global maximum and ξ^{ZF} is increasing for $M<M_{max}$ and decreasing for $M>M_{max}$. Thus M_{max} is the unique optimal M to attain a maximum ξ^{ZF}.

APPENDIX E
PROOF OF PROPOSITION 7

This result can be proved similarly to the proof of proposition 6 by changing the differentiation variable from M to $\bar{p}$. Accordingly we can parameterize a,b,c,d as $1,(M-K),(Kp^{UE}+p^{Coup}+Mp^{BS}),KTr[\mathbf{\Sigma}_M^{-1}]\left(\frac{\zeta^{UL}}{\eta^{UL}}+\frac{\zeta^{DL}}{\eta^{DL}}\right)$ respectively. The quasi-concavity of $\xi^{ZF}(\bar{p})$ follows accordingly similar to the proof in Appendix D. Hence, the local maximum will also be the global maximum which can be found by setting the first derivative to zero, i.e.,

$$\frac{\partial\xi^{ZF}(\bar{p})}{\partial\bar{p}}=0. \tag{75}$$

Solving (75) in a way similar to Appendix D, we obtain the desired result. The details are omitted due to space limitations.

REFERENCES

[1] H. Q. Ngo, E. G.Larsson and T. L.Marzetta, "Energy and Spectral Efficiency of Very Large Multiuser MIMO Systems", *IEEE trans. on Communications*, Vol. 61, No. 4, Apr 2013.

[2] T. L. Marzetta, "Noncooperative cellular wireless with unlimited numbers of base station antennas", *IEEE Trans. Wireless Communications*, Vol. 9, No. 11, pp. 3590-3600, Nov 2010.

[3] F. Rusek, D. Persson, B.K. Lau ; E.G. Larsson, "Scaling up MIMO: opportunities and challenges with very large arrays", *IEEE Signal Processing Magazine*, Vol.30, No.1, pp. 40-60, Jan. 2013.

[4] 3GPP technical specifications group radio access network, Further Advancements for E-UTRA; LTE-Advanced feasibility studies in RAN WG4, 3GPP TR 36.815, March 2010.

[5] Rhodes and Schwarz, "WLAN 802.11n: From SISO to MIMO", 2010.

[6] J. Hoydis, K. Hosseini, S.T. Brink, and M. Debbah, "Making Smart Use of Excess Antennas: Massive MIMO, Small Cells, and TDD", Bell Labs Technical Journal 18(2), 5-21, 2013.

[7] E. Bjornson, L. Sanguinetti, J. Hoydis and M. Debbah, "Optimal Design of Energy-Efficient Multi-User MIMO Systems: Is Massive MIMO the Answer?", *IEEE Transactions on Wireless Communications*, Vol.14, No.6, pp. 3059-3075, June 2015.

[8] C. Masouros, M. Sellathurai and T. Ratnarajah, "Large-Scale MIMO Transmitters in Fixed Physical Spaces: The effect of transmit Correlation and Mutual Coupling", *IEEE trans. Communications*, Vol. 61, No. 7, Jul 2013.

[9] C. A Balanis, *Antenna Theory: Analysis and Design*, 3rd edition.

[10] I. J. Gupta, and A. A. Ksienski, "Effect of Mutual Coupling on the Performance of Adaptive Arrays", *IEEE trans. on Antennas and Propagation*, Vol. AP-31, No. 5, Sep 1983.

[11] Y .Qiaowei, C. Qiang, K. Sawaya, "Performance of adaptive array antenna with arbitrary geometry in the presence of mutual coupling," *IEEE trans on Antennas and Propagation*, Vol. 54, No. 7, pp. 1991-1996, July 2006.

[12] Y. P. Xi, D. G. Fang, Y. X. Sun, Y. L. Chow, "Mutual coupling in a linear dipole array of finite size," *IEEE proc on Microwaves, Antennas and Propagation*, Vol. 152, No. 5, pp. 324-330, Oct. 2005.

[13] T. Svantesson, "The effects of mutual coupling using a linear array of thin dipoles of finite length," *IEEE SP Workshop on Statistical Signal and Array Processing*, Vol. 232, No. 235, pp. 14-16, Sep 1998.

[14] R. Janaswamy, "Effect of element mutual coupling on the capacity of fixed length linear arrays," *IEEE letters on Antennas and Wireless Propagation*, Vol. 1, No. 1, pp. 157-160, 2002.

[15] J. A. G. Malherbe, "Analysis of a linear antenna array including the effects of mutual coupling," *IEEE trans on Education*, Vol. 32, No. 1, pp. 29-34, Feb 1989.

[16] Y. Dawei, F. W. Vook, T. A. Thomas, D. J. Love, A. Ghosh, "Kronecker product correlation model and limited feedback codebook design in a 3D channel model,"*IEEE International Conference on Communications*, Vol. 5865, No. 5870, pp.10-14, June 2014.

[17] X. Artiga, B. Devillers, J. Perruisseau-Carrier, "Mutual coupling effects in multi-user massive MIMO base stations," *IEEE International Symposium on Antennas and Propagation Society*, Vol. 1, No. 2, pp. 1-2, Jul 2012.

[18] B. Clerckx, C. Craeye, D. V-Janvier and C. Oestges, "Impact of Antenna Coupling on 2×2 MIMO Communications", *IEEE trans. on Vehicular Technology*, Vol. 56, No. 3, May 2007.

[19] Z. Li, Z. Du, M. Takahashi, K. Saito and K. Ito, "Reducing Mutual Coupling of MIMO Antennas With Parasitic Elements for Mobile Terminals", *IEEE trans. on Antennas and Propagation*, Vol. 60, No. 2, Feb 2012.

[20] D. F. Kelley and W. L. Stutzman, "Array antenna pattern modeling methods that include mutual coupling effects", *IEEE trans. on Antennas and Propagation*, Vol. 41, No. 12, pp. 1625-1632, Dec. 1993.

[21] S. Chui, A. J.Goldsmith and A. Bahai, "Energy-Efficiency of MIMO and Cooperative MIMO Techniques in Sensor Networks", *IEEE journal on selected areas in Communications*, Vol. 22, No. 6, Aug 2004.

[22] S. Tombaz, and A. Vastberg and J. Zander, "Energy-and Cost-Efficient Ultra-High-Capacity Wireless Access",*IEEE Wireless Communications magazine*, Vol. 18, No. 5, pp. 18-24, 2011.

[23] D. Ha, K. Lee and J. Kang, "Energy Efficiency Analysis with Circuit Power Consumption in Massive MIMO Systems", *IEEE International Symposium on Personal, Indoor and Mobile Radio Communications*, 2013.

[24] G. Miao, "Energy-Efficient Uplink Multi-User MIMO", *IEEE trans. on Wireless Communications*, Vol. 12, No. 5, May 2013.

[25] T. Ratnarajah and R. Vaillancourt, "Quadratic Forms on Complex Random Matrices and Multiple-Antenna Systems", *IEEE Trans. on Information Theory*, Vol. 51, No. 8, pp. 2979-2984, Aug. 2005.

[26] S. Pillai, T. Suel, and S. Cha, "The Perron-Frobenius theorem: some of its applications", *IEEE Signal Processing Magazine*, Vol. 22, No. 2, pp. 62-75,2005.

[27] D. K.Nagar, and A. K.Gupta, "Expectations of functions of complex Wishart Matrix", *Springer Science+Business Media*, 2011.

[28] A. Fehske, G. Fettweis, J. Malmodin, G. Biczok, "The global footprint of mobile communications: The ecological and economic perspective," *IEEE Communications Magazine*, Vol.49, No.8, pp. 55-62, Aug 2011.

[29] J. Hoydis, S. Ten Brink, M. Debbah, "Massive MIMO in the UL/DL of Cellular Networks: How Many Antennas Do We Need?," *IEEE Journal on Selected Areas in Communications*, Vol.31, No.2, pp. 160-171, Feb 2013.

[30] G. Miao, N. Himayat, G.Y. Li, S. Talwar, "Distributed Interference-Aware Energy-Efficient Power Optimization,"*IEEE Transactions on Wireless Communications*, Vol.10, No.4, pp. 1323-1333, April 2011.

[31] D. Nguyen, Le-Nam Tran, P. Pirinen, M. Latva-Aho, "Precoding for Full Duplex Multiuser MIMO Systems: Spectral and Energy Efficiency Maximization," *IEEE Transactions on Signal Processing* , Vol. 61, No.16, pp. 4038-4050, August 2013.

[32] A. C. Cirik, Rui Wang, Yue Rong, Yingbo Hua, "MSE-Based Transceiver Designs for Full-Duplex MIMO Cognitive Radios," *IEEE Transactions on Communications*, Vol. 63, No. 6, pp. 2056-2070, June 2015.

[33] D. N. C. Tse and P. Viswanath, Fundamentals of Wireless Communications, Cambridge University Press, 2005.

[34] S. Boyd and L. Vandenberghe, Convex Optimization, Cambridge University Press, 2004.

[35] Y. Chen, S. Zhang, S. Xu and G. Li, "Fundamental trade-offs on green wireless networks, *IEEE Communications Magazine*, Vol. 49, No. 6, pp. 30-37, 2011.

[36] R. Kumar, J. Gurugubelli, "How green the LTE technology can be?" *International conference on Wireless Communication, Vehicular Technology, Information Theory and Aerospace and Electronic Systems Technology*, pp. 1-5, 2011.

[37] E. Wolfstetter, Topics in Microeconomics: Industrial Organization, Auctions and Incentives, Cambridge University Press, 1999.

[38] A. C. Cirik, R. Wang, Y. Hua, and M. Latva-aho "Weighted sum-rate maximization for full-duplex MIMO interference channels,"*IEEE Transactions on Communications*, Vol. 63, No. 3, pp. 801-815, March. 2015.

[39] S. Huberman and T. L. Ngoc, "MIMO Full-Duplex Precoding: A joint beamforming and self-interference cancellation srtucture," *IEEE Transactions on Wireless Communications*, Vol. 14, No. 4, pp. 2205-2217, Apr. 2015.

[40] A. Abdel Khalek, L. Al-Kanj, Z. Dawy, and G. Turkiyyah, "Optimization Models and Algorithms for Joint Uplink/Downlink UMTS Radio Network Planning with SIR-Based Power Control,"*IEEE Transactions on Vehicular Technology*, Vol. 60, pp. 1612-1625, May 2011.

Sudip Biswas received the B.Tech. degree in Electronics and Communication Engineering from the Sikkim Manipal Institute of Technology, Sikkim, India in 2010 and the M.Sc. degree in Signal Processing and Communications from the University of Edinburgh, Edinburgh, UK in 2013. He is currently working toward the Ph.D. degree in digital communications at the University of Edinburgh's Institute for Digital Communications. His research interests include various topics in wireless communications and network information theory with particular focus on stochastic geometry and possible 5G technologies such as Massive MIMO, mmWave and Full-Duplex.

Christos Masouros (M'06, SM'14), is currently a Lecturer in the Dept. of Electrical & Electronic Eng., University College London. He received his Diploma in Electrical & Computer Engineering from the University of Patras, Greece, in 2004, MSc by research and PhD in Electrical & Electronic Engineering from the University of Manchester, UK in 2006 and 2009 respectively. He has previously held a Research Associate position in University of Manchester, UK and a Research Fellow position in Queen's University Belfast, UK.

He holds a Royal Academy of Engineering Research Fellowship 2011-2016 and is the principal investigator of the EPSRC project EP/M014150/1 on large scale antenna systems. His research interests lie in the field of wireless communications and signal processing with particular focus on Green Communications, Large Scale Antenna Systems, Cognitive Radio, interference mitigation techniques for MIMO and multicarrier communications. He was awarded the Best Paper Award in IEEE GlobeCom 2015. He is an Associate Editor for IEEE Communications Letters.

Tharmalingam Ratnarajah (A'96-M'05-SM'05) is currently with the Institute for Digital Communications, University of Edinburgh, Edinburgh, UK, as a Professor in Digital Communications and Signal Processing. His research interests include signal processing and information theoretic aspects of 5G wireless networks, full-duplex radio, mmWave communications, random matrices theory, interference alignment, statistical and array signal processing and quantum information theory. He has published over 270 publications in these areas and holds four U.S. patents. He is currently the coordinator of the FP7 projects HARP (3.2M) in the area of highly distributed MIMO and ADEL (3.7M) in the area of licensed shared access. Previously, he was the coordinator of FP7 Future and Emerging Technologies project CROWN (2.3M) in the area of cognitive radio networks and HIATUS (2.7M) in the area of interference alignment. Dr Ratnarajah is a Fellow of Higher Education Academy (FHEA), U.K., and an associate editor of the IEEE Transactions on Signal Processing.